JOURNAL OF combinatorial CHEMISTRY

Subscriber access provided by American Chemical Society

Article

Physical Vapor Deposition Method for the High-Throughput Synthesis of Solid-State Material Libraries

Samuel Guerin, and Brian E. Hayden

J. Comb. Chem., **2006**, 8 (1), 66-73• DOI: 10.1021/cc050117p • Publication Date (Web): 03 December 2005

Downloaded from http://pubs.acs.org on March 22, 2009

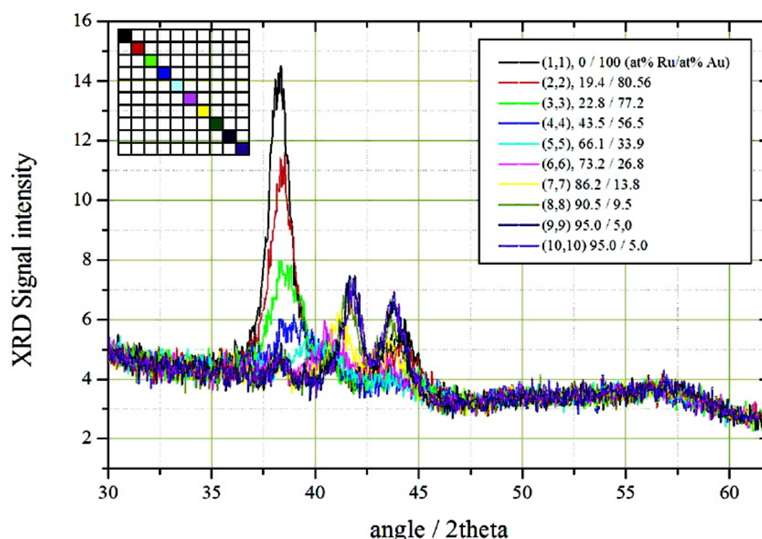

More About This Article

Additional resources and features associated with this article are available within the HTML version:

- Supporting Information
- Links to the 8 articles that cite this article, as of the time of this article download
- Access to high resolution figures
- Links to articles and content related to this article
- Copyright permission to reproduce figures and/or text from this article

View the Full Text HTML

ACS Publications
High quality. High impact.

Journal of Combinatorial Chemistry is published by the American Chemical Society. 1155 Sixteenth Street N.W., Washington, DC 20036

Physical Vapor Deposition Method for the High-Throughput Synthesis of Solid-State Material Libraries

Samuel Guerin and Brian E. Hayden*

School of Chemistry, University of Southampton, Southampton, SO17 1BJ, UK

Received September 8, 2005

A method that combines coevaporation of pure elements from multiple finite-size sources on temperature-controlled substrates with independently controlled source shutters has been used for the synthesis of solid-state material combinatorial libraries. The source shutters are positioned to achieve a controlled gradient of the deposited elements across the substrate and are fixed during the course of deposition. Choice of the shutter position and the rate of deposition for each source allow the direct synthesis of continuous and controlled materials of varying composition. There are significant advantages of the method over alternatives which rely on sequential deposition and subsequent heat treatment to produce thin film materials. The parameters governing the creation of gradients have been identified and defined. Simulations and experimental data have been compared in the case of a single source. Results are presented for the synthesis of a ternary alloy library to demonstrate the methodology.

Introduction

In the past 15 years, combinatorial methods of synthesis and screening have revolutionized the discovery of active compounds in pharmaceutical research and development, and more recently, attention has been turned to the development of combinatorial and high-throughput (HT) methods for the discovery of inorganic and solid-state materials. A promising method of controlled synthesis has been to use physical vapor deposition (PVD) to produce libraries of thin film materials. However, as early as 1965, there was some interest in synthesizing inorganic thin films of two or three elements for which the elemental composition varied spatially across the substrate,[1−3] with the objective of synthesizing a range of compositions for further characterization. Methods of coevaporation of elements from various sources in a vacuum were applied in these investigations and continue to be applied directly[4−7] or with specific modifications[5,6,8−12] to optimize the synthesis for high-throughput applications.

As in the case of screening, the synthetic methodology can be “fast sequential” or truly parallel, and both limits have been applied to the synthesis of thin film materials with a two-dimensional spread of compositions using PVD methods. Sequential PVD methods have been developed most recently and can broadly be divided into two groups. The first of these employs the use of a series of combinatorial shadow masks, either binary, quaternary, or “user-defined” masks,[8−11,13] with sequential deposition of material in each mask arrangement. More recently, the sequential synthesis of inorganic thin film libraries has been achieved using a moving shutter, placed in the vicinity of the substrate, to achieve a gradient of a given material. Subsequent deposition of the other elements is carried out using the same method to create a layered material of varying net composition. Most often, this approach is followed by a heat treatment to achieve a mixing of the elements.[8,12,14−19] An improvement, in which subatomic or monoatomic layers of the various elements are deposited sequentially, has been reported.[13,19−24] This allows direct intimate mixing of the elements and fine control for the synthesis of inorganic materials, such as perovskites of variable composition, but has the inherent disadvantage of any atomic layer methodology in that it is time-consuming for producing bulk thin film material.

A parallel method of PVD synthesis employs the simultaneous deposition of the component elements from multiple sources. The first such reported method in 1965 by Kennedy et al.[1] was developed for the rapid determination of ternary-alloy phase diagrams and employed the use of three off-axis e-beam sources for deposition on a triangularly shaped substrate. The compositional spread of material, or graded profiles, were obtained by taking advantage of the natural profile of the sources which, using the right conditions, can give an uneven deposit of each element across the surface. The compositional spread of the three elements was obtained controlling the relative rate of evaporation of each element. This and subsequent approaches employing co-deposition take advantage of the deposition profile of off-axis PVD sources for simultaneous deposition using relative deposition rate to control compositional ranges without the use of masks, either moving, fixed, or shadow masks.[1−6]

We describe a method for the synthesis of combinatorial libraries using a novel, parallel co-deposition method. The method not only has the advantages of speed, simplicity, and with control of the compositional ranges, but also the simultaneous deposition of the elements to form the material has a number of important advantages over the sequential method. These include the synthesis of wide ranges of composition in nonequilibrium phases ideal for high-throughput screening and the synthesis of, for example, mixed oxides, hydrides, and nitrides.

* Corresponding author. E-mail: beh@soton.ac.uk.

10.1021/cc050117p CCC: $33.50 © 2006 American Chemical Society
Published on Web 12/03/2005

Experimental Section

Experiments have been carried out in an ultrahigh vacuum (UHV) system, base pressure 1×10^{-10} mBar consisting of two cryopumped PVD chambers, an ion-pumped surface analysis and reaction chamber, and a turbomolecularly pumped LPCVD chamber specifically designed to carry out high-throughput synthesis of thin film materials. Facilities for mask transfer and a fast entry port are incorporated, and the synthesis and analysis chambers are interconnected by a series of ion-pumped transfer tubes for substrates of up to 4 in. in diameter. The experiments described here have been carried out in a PVD chamber incorporating six off-axis sources, three e-beam and three Knudsen, cryopanels and shields, a manipulator with heating in the range 300−900K, quartz crystal monitors for e-beam sources, and a number of shutters for the control of material deposition. Shutters and source temperatures are computer-controlled to allow automated deposition of predetermined thicknesses and composition gradients of the thin film materials.

The substrates were (~32 mm)^2, either silicon or silicon nitride-covered silicon (200 nm LPCVD Si_3N_4 on 50-nm thermally grown SiO_2). The deposited materials used were Pt, Au, Ru, and Pd (99.5% from Goodfellow) and Sb, Ge, and Te (99.999% from Alfa Aesar). The thermal evaporators used were standard K-cells (T_{max} = 1400 °C, crucible volume 40 cm^3), high-temperature K-cells (T_{max} = 2000 °C, crucible volume 10 cm^3), or an e-beam evaporator (crucible volume 40 cm^3, model SIHF-270-single earth from Temescal). The crucibles and crucible liners used were either pyrolytic graphite, pyrolytic boron nitride (Sintec Keramik), alumina (Almath Crucibles) and graphite, or Fabmate (Kurt Lesker).

Results and Discussion

Point sources are difficult to apply to the simultaneous deposition of graded materials, since one must rely on the variation of flux as a function of distance; the result is a serious constraint of deposition geometry and substrate size. Practical PVD sources have finite dimensions, usually in the range 1−3 cm, and this has been used to advantage when preparing graded materials. The imposition of fixed shutter to partially shadow the source can be optimized to produce fluxes which vary across the substrate, and this shadowing effect, analogous to the preumbra shadowing of a finite light source, can be used to control a deposition profile. Depending upon the shutter's position within the molecular beam, the gradient can be controlled from the natural profile of the source (which has been optimized to give profiles that are as uniform as possible without using rotation of the substrate) to a fully controlled gradient. The position of the shutter between the substrate and the source is crucial to achieve controlled deposition profiles. If chosen correctly, placement of the shutter in the orthogonal plane controls the profile through a partial masking of the source. Each source profile is controlled independently using its own shutter so that each material can be evaporated with its own gradient. We refer to such deposition as "wedge" growth, and these fixed shutters as "wedge" shutters because of the deposition profile they achieve. Using the wedge growth method on several sources simultaneously and controlling the intrinsic source fluxes allows the deposition of a thin film of variable composition as a function of position across the sample. Sources may be combined out of plane, and mixed compositions of a large number of elements are achievable. This methodology is ideal for high-throughput thin film materials synthesis.

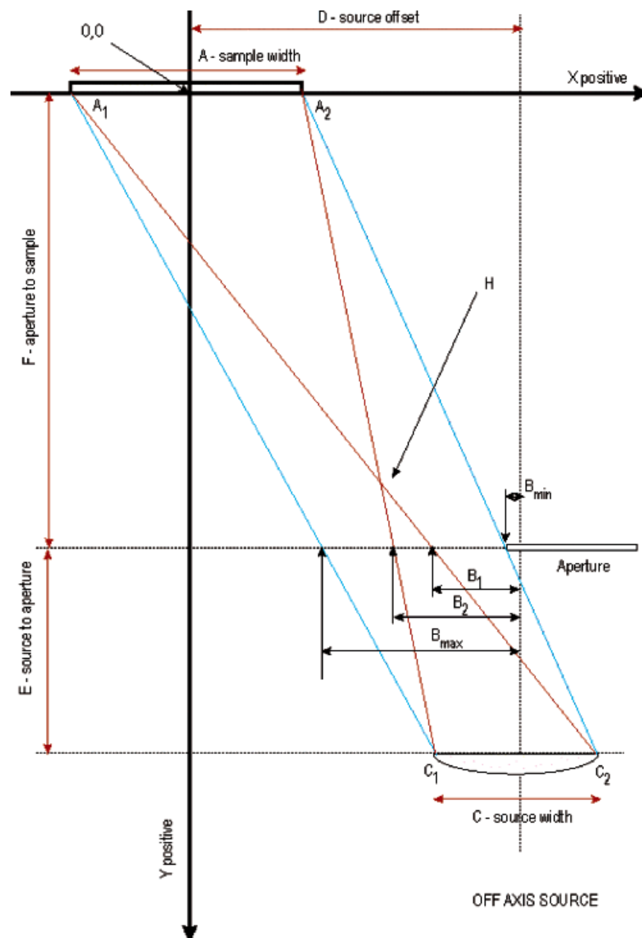

Figure 1. Schematic representations of a single off-axis source and the substrate showing the parameters relevant to the control for the production of graded thin film materials.

Modeling the Finite PVD Source. To establish the conditions required for optimal wedge growth, deposition has been simulated for a number of geometries for a single finite size source. The simulation was implemented using Visual Basic 6, and assumes that the flux at the sample (y) is given by $y = A/r^2$ where A is the power factor and r is the distance between a point on the source and a point on the substrate. Simulations are presented for a source providing constant flux across its finite face, although this can be modified to include variations across the face of the source in the cases of, for example, locally heated e-beam sources. The simulation is carried out in two dimensions, since it provides sufficient detail to predict the wedge growth. Figure 1 shows the detailed geometric arrangement, defined lengths, and positions of a typical "off-axis" source. It should be noted, however, that similar effects are achieved with an on-axis source. The origin to which distances are referenced (0, 0) is defined as the center of the substrate face.

For the purpose of describing the deposition conditions and properties, the following points and distances have been

defined. All distances are given in millimeters unless otherwise stated. A refers to the substrate size. A_1 and A_2 are the two extremities of the substrate. B is the offset of wedge shutter with respect to the axis center of the source. In Figure 1, the wedge shutter is shown in the position B_{min}. C is the source size and C_1 and C_2 are the extremities of the source. D is the offset of the source with respect to the substrate. E is the distance between the source and the wedge shutter, and F is the distance between the wedge shutter and the substrate.

Four points of interest can be defined for the position of the wedge shutter in x with respect to the projected flux of the source. They correspond to the intersection of the wedge shutter with the line of sight of the extremities of the source and substrate (lines AC). Those four points have been defined as B_{min}, B_1, B_2, and B_{max}, The position of the wedge shutter corresponding to these positions can be calculated from geometric considerations.

B_{min} is defined as the point at which the wedge shutter cuts the line A_2C_2, and its position in x with respect to the center of the source is given by

$$B_{min} = \frac{1}{2}\left[\frac{(A - 2D)E + CF}{(E + F)}\right]$$

B_{max} is defined as the point at which the wedge shutter cuts the line A_1C_1, and its position in x with respect to the center of the source is given by

$$B_{max} = -\frac{1}{2}\left[\frac{(A + 2D)E + CF}{(E + F)}\right]$$

B_1 is defined as the point at which the wedge shutter cuts the line A_1C_2, and its position in x with respect to the center of the source is given by

$$B_1 = -\frac{1}{2}\left[\frac{(A + 2D)E - CF}{(E + F)}\right]$$

B_2 is defined as the point at which the wedge shutter cuts the line A_2C_1, and its position in x with respect to the center of the source is given by

$$B_2 = -\frac{1}{2}\left[\frac{(2D - A)E + CF}{(E + F)}\right]$$

A further point of interest, H, can be identified and is defined as the intersection of the two source flux lines A_1C_2 and A_2C_1. The coordinates of point H (H_x, H_y) with respect to the point of origin (the point of origin being the center of the substrate face 0, 0) are given by

$$H_x = \frac{AD}{A + C} \quad H_y = \frac{(E + F)A}{A + C}$$

Wedge growth of various qualities is achieved by using an wedge shutter that cuts the direct path between the source and the substrate, that is, the quadrilateral defined by $A_1A_2C_2C_1$ in the 2D projection (Figure 1). Simulations show that the triangle defined by H, C_1, and C_2 gives the region in which the wedge shutter cutting the source flux will give rise to linear gradients across the *entire* substrate. For a wedge shutter which cuts the flux in all other positions, incomplete or no wedge growth is obtained. In summary,

For F > H_y, $B_{min} > B_1 > B_2 > B_{max}$ if:

$B > B_{min}$ uniform film (natural profile of unimpeded source)

$B_{min} > B > B_1$ partial gradient across sample (plateau + gradient)

$B_1 > B > B_2$ linear gradient across whole sample

$B_2 > B < B_{max}$ partial gradient across sample (gradient + no deposition)

$B_{max} > B$ no deposition

For $F < H_y$, $B_{min} > B_2 > B_1 > B_{max}$ if:

$B > B_{min}$ uniform film (natural profile of unimpeded source)

$B_{min} > B > B_2$ partial gradient across sample (plateau + gradient)

$B_2 > B > B_1$ partial gradient across sample (plateau + gradient + no deposition)

$B_1 > B > B_{max}$ partial gradient across sample (gradient + no deposition)

$B_{max} > B$ no deposition

Table 1. Results of the Simulation Showing the Effect of Moving the Wedge Shutter Position (Figure 1) on the Profile of the Deposited Material for the Case of a Single Source

B mm	max flux, %	min flux, %	mormalized gradient, %	predicted profile
−59	0	0	0−0	no deposit
−58	5.86	0	0−100	no deposit + gradient
−57	12.69	0	0−100	no deposit + gradient
−56	19.51	0	0−100	no deposit + gradient
−55	26.32	0	0−100	no deposit + gradient
−54	34.08	0	0−100	no deposit + gradient
−53	40.86	0	0−100	linear gradient
−52	47.63	4.00	8.4−100	linear gradient
−51	54.39	11.00	20.22−100	linear gradient
−50	61.13	17.98	29.42−100	linear gradient
−49	67.87	24.96	36.77−100	linear gradient
−48	74.59	31.92	42.80−100	linear gradient
−47	82.26	38.87	47.26−100	linear gradient
−46	88.96	45.82	51.51−100	linear gradient
−45	95.64	53.74	56.19−100	linear gradient
−44	97.77	60.66	62.05−100	linear gradient
−43	98.18	67.57	68.82−100	plateau + gradient
−42	98.59	74.47	75.53−100	plateau + gradient
−41	99.00	81.3	82.18−100	plateau + gradient
−40	99.41	88.24	88.76−100	plateau + gradient
−39	99.70	95.10	95.38−100	plateau + gradient
−38	100.00	97.55	97.55−100	natural profile of source

Table 1 shows the results of a simulation for a specific growth geometry, calculating the expected deposition profiles for the wedge shutter moving across the full range of the source flux to the sample. The fixed values (in mm) used were $A = 22$, $C = 20$, $D = 162$, $E = 150$,and $F = 350$. This gives $B_{min} = -38.3$, $B_1 = -44.9$, $B_2 = -52.3$ and $B_{max} = -58.9$. "Maximum flux" is defined as the maximum percentage of source material deposited on the substrate with respect to the amount of material that would have been deposited had no wedge shutter been used. "Minimum flux" is defined as the minimum percentage of material deposited on the substrate with respect to the amount of material that would have been deposited had no wedge shutter been used. The "normalized gradient" corresponds to the percentage

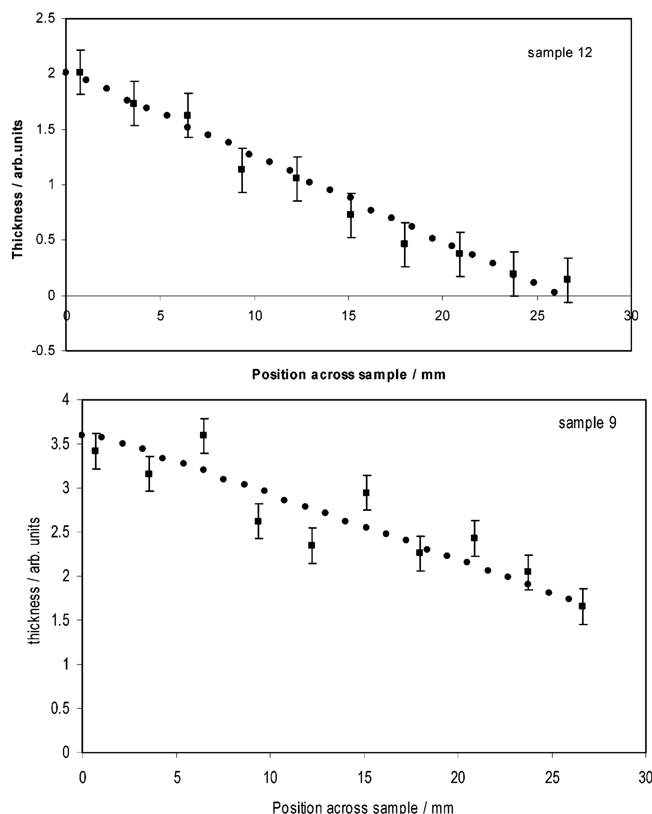

Figure 2. Graphs showing the results of the simulation of the deposition profile from a single PVD Knudsen source. The associated dimensions were $C = 20$ mm, $A = 26$ mm, $E = 350$ mm, $F = 150$ mm, and $D = 162$ mm (see Figure 1). Simulations are shown for the cases of $B = -51.8$ and -45 mm. Experimental data of thin films of gold deposited on a silicon nitride substrate synthesized with these parameters is also shown.

difference between the maximum and minimum amounts deposited across the sample. Note that the deposition (the way this normalized gradient is deposited) does not always take place in a continuous gradient (labeled linear gradient) across the sample.

Comparison of Modeled PVD Profile with Experiment. Figure 2 shows the results of simulations and corresponding experimental data for the deposition of gold on a SiN substrate. Results are shown in the direction of deposition (i.e., the main diagonal of the square substrate where the Au content had the most variation). In the direction orthogonal to this line, the deposition profile will reflect that of the natural source profile, which in this case is very nearly invariant. The source was a Knudsen cell with dimension $C = 20$ mm, $A = 26$ mm, $E = 350$ mm, $F = 150$ mm, and $D = 162$ mm. B was set for the 2 examples at $B = -51.8$ mm for sample 9, and $B = -45$ mm for sample 12. It is clear that there is good correlation between simulated and experimental data.

The effect of moving the position of the wedge shutter on the profile of the deposited material can be seen in Figure 3. Four depositions of the same material varying only the position of the wedge shutter and the time of deposition have been performed. It is clear from the four graphs that as the position is increased from 60 to 75%, the profile of the deposited material varies from a plateau + gradient to a gradient + no deposit with a region between where a full wedge is obtained. This is in agreement with the model proposed and with the simulations summarized in Table 1. It should be noted that increasing the position of the wedge shutter from 60 to 65% still gives rise to a plateau + gradient region; however, the plateau is smaller for the 65% wedge shutter position, and accordingly, the gradient is larger.

Multiple PVD Sources. One considerable advantage of producing the deposition profile in this way is that not only is the profile controllable, but also it can be defined for a number of sources independently for simultaneous deposition of multicomponent materials. The maximum number of sources that can be used for co-deposition depends only on the geometry, the size of the vacuum chamber, and the physical size of sources. We have designed a HT-PVD materials fabrication system which incorporates two HT-PVD growth chambers. One of these has four sources arranged in 4-fold symmetry, and the second has six sources arranged in 6-fold symmetry. Using this method in the second chamber, up to six elements can be deposited simultaneously with control of composition and thickness. Each element can be deposited with a gradient varying from the limits of 0−100% to that constrained by the natural profile of the source over the substrate (i.e., 97−100%). The gradient of each source can be adjusted independently of the other sources. To obtain the desired gradient, the shutter is moved to the appropriate position before evaporation; therefore, there are no moving parts during evaporation. To achieve the required final spread of composition, the evaporation rate of each source is set appropriately and kept constant during the deposition cycle.

Figure 4 shows a typical ternary composition spread of Pd, Pt, and Au. Each element was deposited using an electron beam source. The three elements were arranged in a 3-fold symmetry (120° apart). Figure 4a, 4b, and 4c show the relative atomic percentages of palladium, gold, and platinum, respectively, measured by energy dispersive spectroscopy (EDS). The deposition was carried out on a $(32\ \text{mm})^2$ square silicon substrate. The substrate temperature during deposition was 300K. A contact mask was used on the substrate to obtain a 10×10 matrix of the various compositions. This mask has been used in this laboratory for the synthesis and subsequent screening of model electrocatalysts on microfabricated arrays of electrodes.[25] Figure 4d is a classical ternary plot showing the different compositions that have been synthesized in the 10×10 matrix. The active area of the Si substrate on which the elements were deposited is 19 mm × 19 mm. Each opening in the contact mask is $1.2 \times 1.2\ \text{mm}^2$ with a separation of 0.8 mm. Therefore, for such an array, it can be expected that in the case of deposition profiles which cover the entire range of compositions, the uniformity of each field within the library is 6.3% and represents the largest compositional variation within a field. Deposition profiles which cover a limited range of the compositional range or a reduction in the field size will result in concomitantly lower ranges of composition within the field.

One of the main advantages of this approach for the synthesis of thin films is the possibility to “zoom into” a region of interest. Figure 5 shows the position of 100 fields

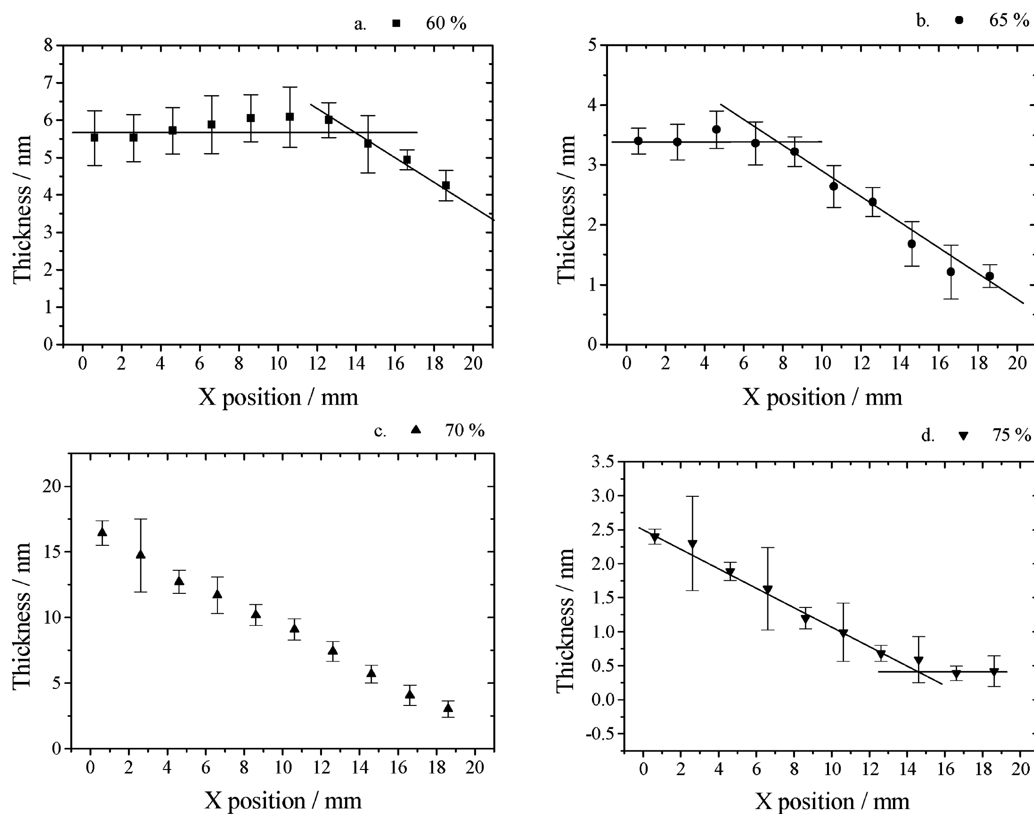

Figure 3. Graphs showing the effect of varying the wedge shutter position on the profile of the deposited thin film for a single source. The percentages of wedge shutter express the position of the wedge shutter with respect to the minimum and maximum positions. The experimental data is for platinum deposited from an e-beam source. The thicknesses have been obtained by ellipsometry.

as measured by EDS in a ternary plot for two different Ge, Sb, and Te ternary libraries (nos. 773 and 777). Library 773 was synthesized with a large spread of compositions ranging from 1 to 60 at. % of Ge, 3 to 75 at. % of Sb, and 2 to 81 at. % of Te. By varying the position of the wedge shutter and the power of the evaporation sources, it is possible to change drastically the compositional domain covered over the surface of the substrate. Library 777 in Figure 5 was synthesized in this way to provide a much more detailed library in a particular compositional range of interest. This time, the compositional spread ranges from 6 to 32 at. % for Ge, 7 to 58 at. % for Sb, and 13 to 72 at. % for Te. Clearly, the compositional range within screened fields in the no. 777 library will be significantly smaller than in no. 773. This ability to control the composition spread provides important versatility in HT synthesis. In addition, confinement of the controlled compositional region to $(\sim 25\ \mathrm{mm})^2$ allows this methodology to be combined with arrays of microfabricated micro electro-mechanical systems (MEMS) for HT materials screening.

Another important aspect of the technique is the reproducibility of the synthesis method. Figure 6 shows two ternary plots of two libraries, nos. 773 and 789, both deposited under identical conditions. It is clear form the spreading of the points on the ternary plot that both arrays cover the same domain of compositional spread. An important aspect of this reproducibility is that the synthesis of the two libraries was nonconsecutive, and 15 other libraries were deposited in the week between their synthesis. Furthermore, the conditions of deposition (i.e., the power and wedge shutter position) had been altered for library synthesis: for example, library no. 777 was synthesized between nos. 773 and 789 with quite different parameters.

Although the ternary plots (Figures 4−6) show the compositions of 100 EDS analyzed fields, a screened library may contain significantly more fields within the overall compositional region if the figure of merit or analysis can be carried out in a small area. This is because the composition of the material synthesized changes smoothly with position, and on a continuous film (or a masked film with 1000 fields, say, rather than 100) the composition between measured points can be calculated. The 100 analyzed (or 10 × 10 masked fields) represented in the ternary plots are only indicative of the compositional domain covered in a potential screened library.

Co-deposition of metals at room temperature provides large compositional ranges of alloy materials both in the bulk and at the surface, since the materials do not require annealing to provide mixing and are in a nonequilibrium state. Therefore, amorphous or crystalline solid solutions can be obtained. Thermodynamic phases and surface segregation accompany the annealing of the sample. Either postdeposition or during deposition, the substrate manipulator can be heated in the range 300−1100K. Figure 7 shows a selection of X-ray diffractograms obtained for a binary library of gold and ruthenium. Ten diffractograms are plotted, each corresponding to one field along the main diagonal of the library. The composition varies from 100 at. % Au/0 at. % Ru to 5 at. % Au/95 at. % Ru. There is a clear change in the intensity and position of the peaks as the composition changes. At 100%

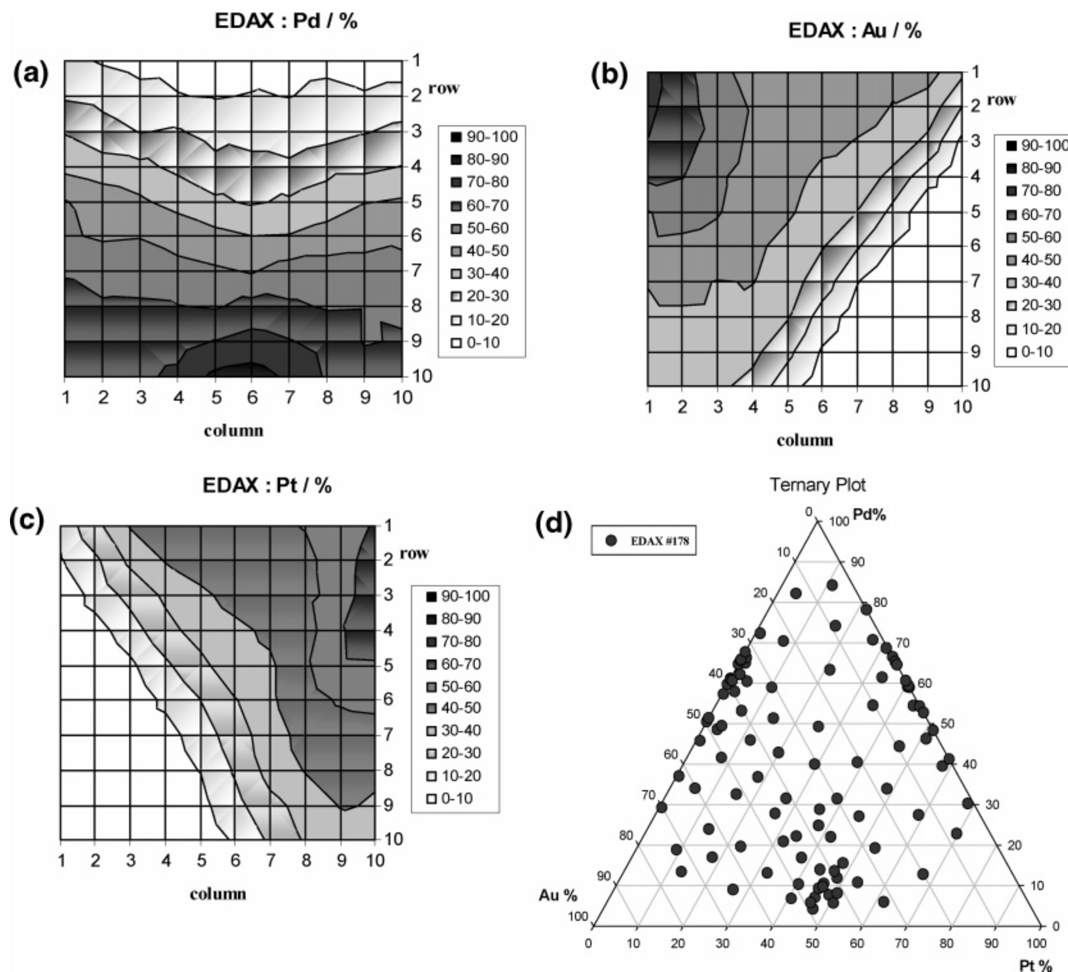

Figure 4. Compositional plots (from EDS) of an alloy synthesized by co-deposition of gold, palladium, and platinum onto a silicon substrate, showing the relative atomic percentages across the substrate of (a) palladium, (b) gold, and (c) platinum. The spread of compositions covered by 100 fields in a (10 × 10) library of this material is shown in (d).

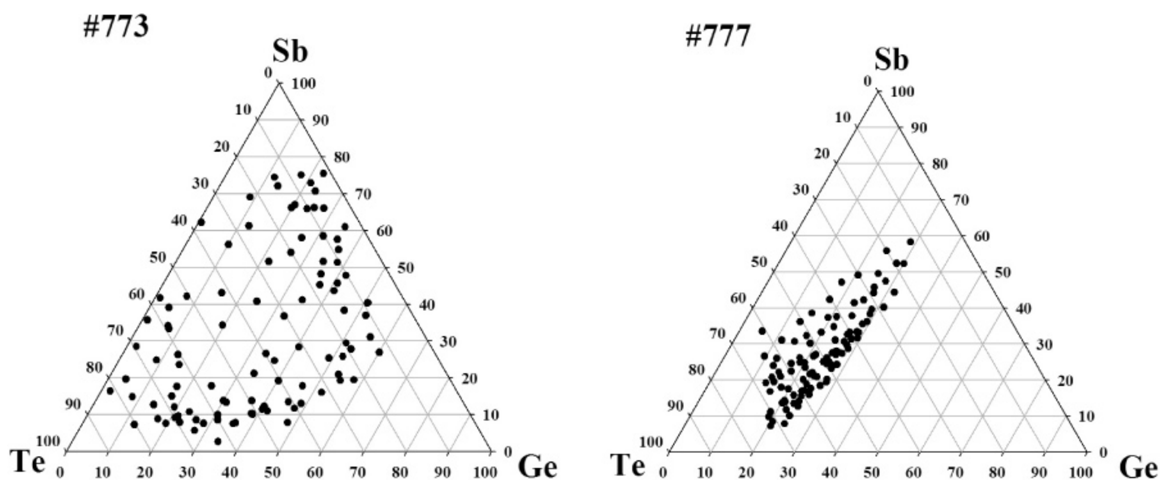

Figure 5. The compositional range of two ternary libraries of Ge, Sb, and Te are shown to emphasize the ability to restrict synthesis to the compositional region of interest. The source used for Ge was a 10 cm^3 high-temperature K-cell and for Sb and Te, 40 cm^3 low-temperature K-cells. Compositional data is expressed in atomic % and has been obtained by EDS.

Au composition, the peak corresponds to the main diffraction of Au in the (225) space group. As the Au is diluted with Ru, the Au peak intensity decreases and continuously shifts, while two other peaks appear which correspond to the hexagonal phase of Ru. No other crystalline phases are observed across the complete compositional range for the room-temperature-deposited materials. These nonequilibrated continuous solutions in the crystalline phase and ranges of amorphous materials provide a powerful tool for screening as a function of elemental composition. Annealing the thin film produces the thermodynamic phases, which can also be investigated but is often less useful as a materials library. In addition, room-temperature deposition also leads to materials with very little or no surface segregation, making

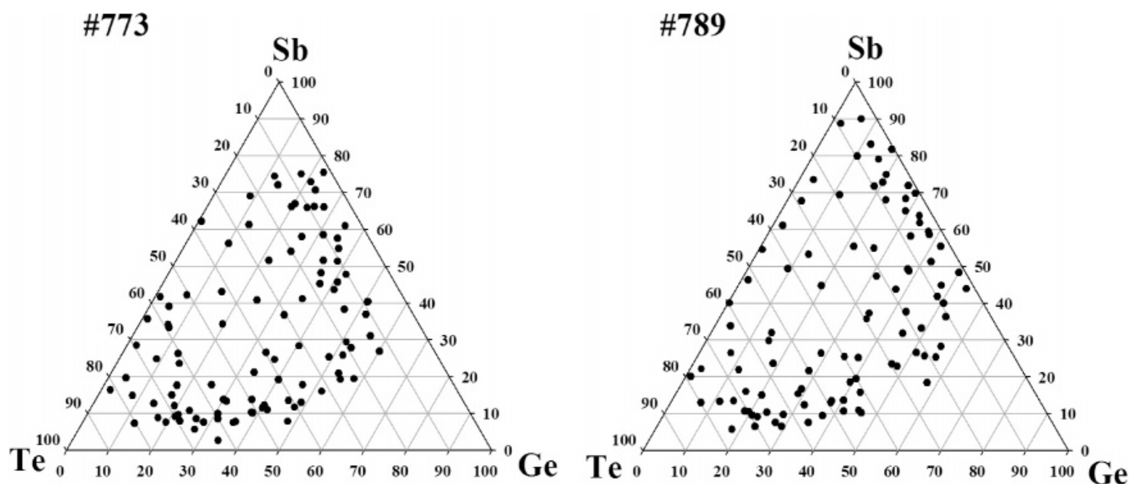

Figure 6. The compositional range of two ternary libraries of Ge, Sb, and Te synthesized using the same deposition parameters are shown to emphasize the reproducibility of the method. The two depositions were carried out more than a week apart, during which time the deposition parameters had been changed significantly to synthesize other libraries. The source used for Ge was a 10 cm^3 high-temperature K-cell and for Sb and Te, 40 cm^3 low-temperature K-cells. Compositional data is expressed in atomic % and has been obtained by EDS.

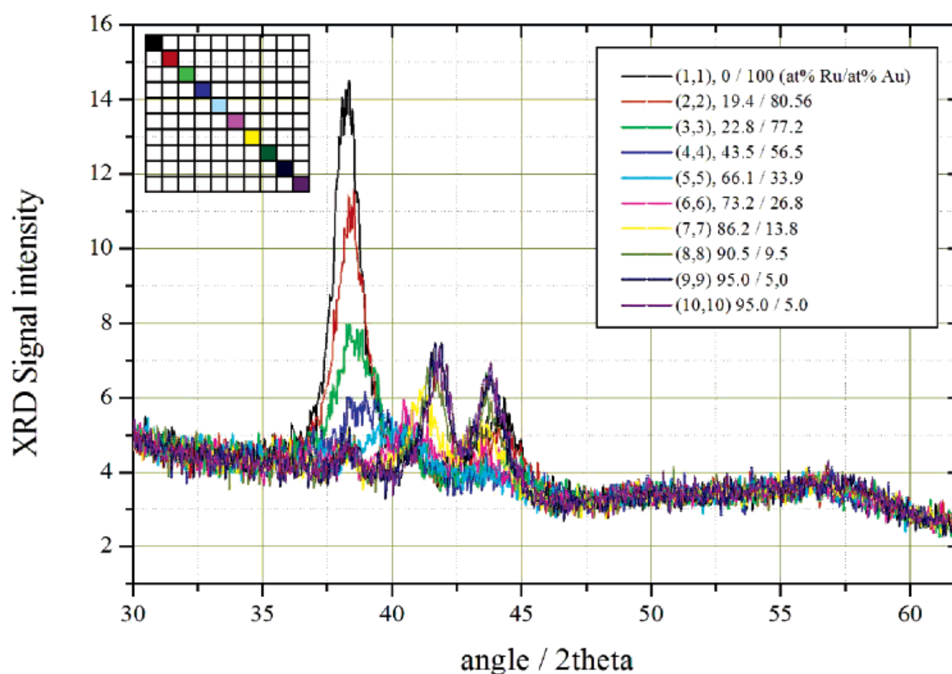

Figure 7. Selected X-ray diffractograms for a Au−Ru binary system deposited on Si showing the effect of the composition on the crystal structure for materials deposited with the substrate at room temperature. Measurements carried out with a Bruker C2 diffractometer, using $Cu_{K\alpha}$ source, $\lambda = 1.541\ 84$ Å.

them ideal for the screening of surface phenomena over wide ranges of composition.[25]

Perhaps an even more significant advantage of the controlled and simultaneous deposition of elements using this method is that when combined with an atom plasma source, the direct HT synthesis of mixed (or doped) oxide, nitride and hydride phases can be achieved. Restricted mobility or stability of such materials generally precludes the application of multiple depositions and annealing to their synthesis.

Conclusion

We report the design of a novel co-deposition method using fixed shutters combined with e-beam and Knudsen PVD sources to produce controlled libraries of a wide compositional range. The deposition profile can be predicted and controlled, and the deposition profile of each source can be varied independently, as can the deposition rate to create the libraries. An experimental system is described which can be used to deposit continuous thin film or discrete masked libraries with up to six components. An example is shown for the deposition of a ternary alloy deposited in a (10 × 10) array using a contact mask. The co-deposition method enables the synthesis of libraries with a large compositional range without the need for heat treatment to achieve the mixing of the components. The advantages of this method for the screening of nonequilibrated metal alloys and the synthesis of mixed metal oxides, nitrides, and hydrides are highlighted.

Acknowledgment. We acknowledge the support of the EPSRC through the JIF scheme (GR/R50639) for the

Combinatorial Centre of Excellence in the School of Chemistry in the University of Southampton. The authors also acknowledge the support of Ilika Technologies Ltd, Dr. Karen Brace, Dr. Claire Mormiche, Dr. Mark Light, and Jens-Peter Suchsland.

References and Notes

(1) Kennedy, K.; Stefansky, T.; Davy, G.; Zackay, V. F.; Parker, E. R. *J. Appl. Phys.* **1965**, *36*, 3808.
(2) Miller, N. C.; Shirn, G. A. *Appl. Phys. Lett.* **1967**, *10*, 86.
(3) Hanak, J. J. *J. Mater. Sci.* **1970**, *5*, 964.
(4) Russek, S. E.; Bailey, W. E.; Alers, G.; Abraham, D. L. *IEEE Trans. Magn.* **2001**, *37*, 2156.
(5) van Dover, R. B.; Schneemeyer, L. F.; Fleming, R. M. *Nature* **1998**, *392*, 162.
(6) Koinuma, H. *Solid State Ionics* **1998**, *108*, 1.
(7) Smith, R. C.; Hoilien, N.; Campbell, S. A.; Roberts, J. T.; Gladfelter, W. L. *Chem. Mater.* **2003**, *15*, 292.
(8) Wang, J. S.; Yoo, Y.; Gao, C.; Takeuchi, I.; Sun, X. D.; Chang, H. Y.; Xiang, X. D.; Schultz, P. G. *Science* **1998**, *279*, 1712.
(9) Briceno, G.; Chang, H.; Sun, X. D.; Schultz, P. G.; Xiang, X.-D. *Science* **1995**, *270*, 273.
(10) Xiang, X. D.; Sun, X. D.; Briceno, G.; Lou, Y. L.; Wang, K. A.; Chang, H. Y.; Wallacefreedman, W. G.; Chen, S. W.; Schultz, P. G. *Science* **1995**, *268*, 1738.
(11) Chang, H.; Gao, C.; Takeuchi, I.; Yoo, Y.; Wang, J.; Schultz, P. G.; Xiang, X. D.; Sharma, R. P.; Downes, M.; Venkatesan, T. *Appl. Phys. Lett.* **1998**, *72*, 2185.
(12) Danielson, E.; Golden, J. H.; McFarland, E. W.; Reaves, C. M.; Weinberg, W. H.; Wu, X. D. *Nature* **1997**, *389*, 944.
(13) Matsumoto, Y.; Murakami, M.; Jin, Z. W.; Ohtomo, A.; Lippmaa, M.; Kawasaki, M.; Koinuma, H. *Jpn. J. Appl. Phys., Part 2* **1999**, *38*, L603.
(14) Yoo, Y.-K.; Duewer, F.; Yang, H.; Yi, D.; Li, J.-W.; Xiang, X.-D. *Nature* **2000**, *406*, 704.
(15) Yoo, Y.-K.; Ohnishi, T.; Wang, G.; Duewer, F.; Xiang, X.-D.; Chu, Y. S.; Mancini, D. C.; Li, Y.-Q.; O'Handley, R. C. *Intermetallics* **2001**, *9*, 541.
(16) Yoo, Y.-K.; Duewer, F.; Fukuruma, T.; Yang, H.; Yi, D.; Liu, S.; Chang, H.; Hasegawa, T.; Kawasaki, M.; Koinuma, H.; Xiang, X.-D. *Phys. Rev. B* **2001**, *63*, 224421.
(17) Chang, H.; Takeuchi, I.; Xiang, X.-D. *Appl. Phys. Lett.* **1999**, *74*, 1165.
(18) Xiang, X.-D. *Appl. Surf. Sci.* **2002**, *189*, 188.
(19) Tsui, F.; Ryan, P. A. *Appl. Surf. Sci.* **2002**, *189*, 333.
(20) Takahashi, R.; Kutoba, H.; Murakami, M.; Yamamoto, Y.; Matsumoto, Y.; Koinuma, H. *J. Comb. Chem.* **2004**, *6*, 50.
(21) Takahashi, R.; Matsumoto, Y.; Koinuma, H.; Lippmaa, M.; Kawasaki, M. *Appl. Surf. Sci.* **2002**, *197*−*198*, 532.
(22) Fukumura, T.; Ohtani, M.; Kawasaki, M.; Okimoto, Y.; Kageyama, T.; Koida, T.; Hasegawa, T.; Tokura, Y.; Koinuma, H. *Appl. Phys. Lett.* **2000**, *77*, 3426.
(23) Koinuma, H.; Kawasaki, M.; Itoh, T.; Ohtomo, A.; Murakami, M.; Jin, Z.; Matsumoto, Y. *Physica C* **2000**, *335*, 245.
(24) Koinuma, H.; Aiyer, H. N.; Matsumoto, Y. *Sci. Technol. Adv. Mater.* **2000**, *1*, 1.
(25) Guerin, S.; Hayden, B. E.; Lee, C. E.; Mormiche, C.; Russell, A. E. *Angew. Chem., Int. Ed.* **2005**, submitted.

CC050117P